Synthesis, molecular modeling, quantum chemical calculations and in silico drug profiling of the novel (4-phenylpiperazin-1-ium) hydrogenfumarate as a tyrosinase inhibitor

Mahdi Jemai, Noureddine Issaoui, Thierry Roisnel, Aleksandr S. Kazachenko, Houda Marouani, Omar Al-Dossary

Synthesis, Molecular Modeling, Quantum Chemical Calculations and InSilico Drug Profiling of the novel (4-phenylpiperazin-1-ium) Hydrogenfumarate as a Tyrosinase Inhibitor

Mahdi Jemai[(a)], Noureddine Issaoui[(b)*],Thierry Roisnel[(c)], Aleksandr S. Kazachenko[d,e], , Houda Marouani[(a)] Omar M. Al-Dossary[f]

(a)Laboratory of Material Chemistry, Faculty of Sciences of Bizerte, University of Carthage, Bizerte, Tunisia

(b)Quantum Physics Laboratory, Faculty of Sciences, University of Monastir, Monastir 5079, Tunisia.

(c)Univ Rennes, CNRS, ISCR (Institut des Sciences Chimiques de Rennes) –UMR 6226, F-350 0 0 Rennes, France

(d) Institute of Chemistry and Chemical Technology SB RAS, Federal Research Center "Krasnoyarsk Science Center SB RAS", Akademgorodok, 50/24, Krasnoyarsk, 660036, Russia

(e) Siberian Federal University, Svobodny av., 79, Krasnoyarsk, 660041, Russia

(f) Department of Physics and Astronomy, College of Science, King Saud University, PO Box 2455, Riyadh 11451, Saudi Arabia.

* Corresponding authors: Noureddine Issaoui, email: issaoui_noureddine@yahoo.fr

ABSTRACT

The complexation between fumaric acid (FA) and 1-phenylpiperazine (1PP) is a fruitful cooperation that allowed the preparation of a new organic crystal entitled (4-phenylpiperazin-1-ium) hydrogenfumarate denoted by 4PPHFUM, which is reported in the present manuscript. This new substance is created by the slow evaporation that occurs when 1-phenylpiperazine and fumaric acid are combined in a stoichiometric 1:1 ratio. The stacking of the crystal is provided by O-H…O, N-H…O and C-H…O hydrogen bonds, also supported by C-H…π interactions between the organic cations. The importance of these interactions in the formation of this new crystal is confirmed by the Hirshfeld surface analysis which showed that H-bonds and supramolecular C-H…π interactions account for about half of the non-covalent interactions existing in this compound. These non-covalent bonds that encompass the synthesis and design of this supramolecule have also been analyzed in detail using a quantum chemical computational study. Using thedocking -based drug design strategy, we investigated the therapeuticeffectof this cooperative outcome between fumaric acid and 1-phenylpiperazine to demonstrate the improved therapeutic property of this novel non-covalent compoundas a tyrosinase inhibitor. 4PPHFUM was found to be a potent tyrosinase inhibitor with high interaction energy with its protein, higher than that of the most potent tyrosinase inhibitors (Thiamidol, Hydroquinone, Resorcinol, Hexylresorcinol and Kojic Acid).

Keywords: 1-phenylpiperazine, Fumaric acid, Single-crystal X-ray diffraction, Hirshfeld surfaces, Quantum chemical calculations, Molecular docking, Tyrosinase Inhibitor.

1. Introduction

The formation of organic salt crystals is the result of interactions between donor and acceptor of hydrogen atoms which result in a transfer of protons allowing the establishment of hydrogen bonds which are the main non-covalent interactions responsible for the attachment between organic entitiesin parallel with other interaction such as C-H···π, N-H···π, π···π stacking and van der Waals (vdW) interactions [1,2]. Crystal engineering is the main branch that offers us an in-depth understanding of these intermolecular interactions, their crystallographic geometry and how we can apply them to the study of the structure of these new solids, which has been the topic of recent articles [3-5]. In the present work, we use fumaric acid as hydrogen donor and 1-phenylpiperazine as hydrogen acceptor.

We cannot talk about fumaric acid without mentioning its role in the development it left in the field of medicine and the Nobel Prize in 1939, the oxidation process of FA acts as a biological catalyst of the cellular respiratory chain in humans with scurvy, a disease caused by vitamin C deficiency, which causes teeth loosening, gum purulence, bleeding, and ultimately death [6].Newly, fumaric acid has also been used as an oral therapy for the treatment of the newest and most dangerous disease, Coronavirus (SARS-CoV-2) [7,8].

Thanks to the structural features of FA commonly associated with the carboxyl function of tyrosinase inhibitors, recent research shows that FA is an effective and safe tyrosinase inhibitor, as presented in the literature [9]. This is why we speculated that complexing FA with another molecule with an interesting therapeutic effect could improve their efficacy against tyrosinase.

Discolorations of fruits, vegetables, as well as hyperpigmentation of human skin are common unwanted phenomena. Tyrosinase is an essential enzyme associated in this enzymatic browning [10]. For the latter reason, researchers and scientists are encouraged to concentrate their efforts on the synthesis and characterization of intense novel tyrosinase inhibitors [10,11]. Tyrosinase inhibitors could be used in health care and beauty products for bleaching and depigmentation, as well as in agriculture as bioinsecticides [12,13].

Piperazine derivatives constitute a class of heterocyclic compounds with pharmacological significance and important implications in medical science [14]. These derivatives are present in a variety well-known drugs with different therapeutic uses for the reason to their interesting pharmacological properties, such as antidepressant and antipsychotic activity [15,16], anticancer activity [17,18], cardiovascular treatments [19], diabetes therapies [20], metabolic

disorders treatments [21], Anti-tuberculosis activity [22] and antiviral agents [23]. For us, the most interesting aspect is the therapeutic activity of piperazine derivatives as tyrosinase inhibitors. Recent research has demonstrated the efficacy of combination with piperazine compounds to produce highly active tyrosinase inhibitors, and that this may provide a valuable basis for the development of new tyrosinase inhibitors candidates [24-26].

The synthesis of the novel organic compound (4-phenylpiperazin-1-ium) hydrogenfumarate is the topic of this manuscript. Fumaric acid and 1-phenylpiperazine interact to create and evaluate the structure of this supramolecule, examine its associated properties and study the improvement brought about by the cooperative effect in this new chemical based on a combined experimental and theoretical study, as well as the estimated therapeutic effect of this innovative material's tyrosinase inhibition.

2. Experimental

2.1. Materials

Fumaric acid and 1-phenylpiperazine were combined in a 1:1 stoichiometric ratio to create the novel organic supramolecular molecule $(C_{10}H_{15}N_2)(C_4H_3O_4)$. The following procedures were used to produce single crystals suitable for X-Ray diffraction: Fumaric acid (116 mg) and 1-phenylpiperazine (0.157 mL) were combined, diluted in ethanol (6 mL) at 25°C, agitated for 40 minutes, and then stored at room temperature. After 10 days, single crystals had been spotted. **Scheme1** illustrates the chemical reaction underlying the synthesis of 4PPHFUM.

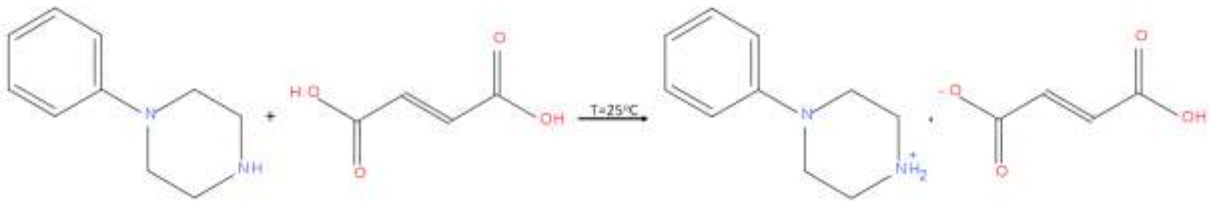

Scheme1. The Production of (4-phenylpiperazine-1-ium) hydrogenfumarate through the chemical interaction of fumaric acid and 1-phenylpiperazine.

2.2. X-ray data collection for crystallographic analysis

The D8 VENTURE Bruker AXS diffractometer equipped with a CCD detector and a monochromatic molybdenum Mo Kα radiation wavelength (λ= 0.71073 Å) as its X-ray source was used to identify the crystallographic parameters of the new compound 4PPHFUM. Using the SADABS program, the multi-scan method was used to correct the data collection [27]. Using SHELXT-2018 method, WINGX program allows us to directly solve the structure, thus

displaying the positions of all atoms except hydrogen atoms followed by refinement using full-matrix least-squares techniques based on F^2 (SHELXL-2018) [28]. A different map was employed to find and then refine the nitrogen hydrogen atoms. With C—H = 0.99 (methylene) and C—H = 0.95 (aromatic) and O-H (hydroxyl) HFIX code 147 and U_{iso}(H) = 1.2U_{eq}(C/O), the remaining H atoms have been taken into account as riding. Crystallographic data and structural refinements are presented in **Table 1**.

2.3. DFT analyses

Theoretical chemists have used their ability to quantifiably simulate non-covalent interactions between organic compounds to estimate their crystal structures and accurately assess their physical properties. This explains the increase in the number of current research papers that rely primarily on this theoretical framework [29-37]. Using Gaussian 09 software, we optimized the structure of this novel compound in gas phase [38,39]. The B3LYP/6-31G(d) method was used for all theoretical computations of the electronic framework and optimized geometry of 4PPHFUM [40]. These theoretical calculations allow us to confirm and better understand the interaction between hydrogenfumarate and 4-phenylpiperazin-1-ium, and to map the role of non-covalent interactions in the maintenance of the crystal edifice using quantum chemical calculations.

3. Results and Discussion

3.1. Structural description and supramolecular characteristics

The asymmetric unit of the title compound is a 1:1 combination of a hydrogenfumarate anion and a 4-phenylpiperazine-1-ium cation, as shown in **Figure 1**. The (4-phenylpiperazine-1-ium) hydrogenfumarate crystallizes in an orthorhombic crystal system with space group $Pca2_1$ and the following lattice parameters: a = 26.609 (3) Å, b = 7.9792 (9) Å, c = 6.6729 (6) Å, V = 1416.8 (2) $Å^3$ and Z = 4. The various geometric distance and angle parameters are presented in **Table 2**. We have projected the structure of 4PPHFUM in the $(\vec{a}, \vec{b})$ plane, which is the plane with the most obvious atomic arrangement, in order to describe its distribution in the crystalline system. This crystal system is formed by symmetry operators, as follows: c-type mirrors perpendicular to $\vec{a}$ parallel to $\vec{b}$ located at x=1/4 and x=3/4; a-type mirrors perpendicular to $\vec{b}$ parallel to $\vec{c}$ placed at y=0 and y=1/2; orientation axes 2_1 parallel to $\vec{c}$ positioned at (0,0,0), (1,0,0), (0,1,0) and (1,1,0). Through creating N-H...O and C-H…O hydrogen bonds between organic cations and hydrogenfumarate anions, a supramolecular network is formed. The 4-phenylpiperazine-1-ium cation appears in layers parallel to the

$(\vec{a}, \vec{b})$ planes at x=0, x=1/2 and x=1, between which the hydrogenfumarate anions are implanted at x=1/4 and x=¾, connected with strong O-H...O type bonds.

This molecular assembly can be defined as a two-dimensional structure resulting from non-covalent interactions between molecules that ensure the coherence and stability of the crystalline system. N-H...O and C-H...O hydrogen bonding are the strongest non-covalent interactions involved in the attachment between anions and cations in this crystal system. As listed in **Table 3**, O-H…O hydrogen bond have a distance of 2.4589 (11) Å between donor and acceptor which proves the strong character, N-H...O hydrogen bonds have an average distance value between donor and acceptor of 2.7 Å, whereas C-H...O hydrogen bonds have a higher distance value and therefore weaker interaction, with a $d_{donor\text{-}acceptor}$ ranging from 3.1853 (14) to 3.3843 (15) Å. These bonds have been redistributed to form a new supramolecular unit of type $R_6^6(21)$ as shown in **Figure 3a** [41]. The criteria for the creation of C-H...π interactions have been satisfied [42]. With distance values of 3.55 and 3.66 Å, this type of interaction has been established between organic cations (**Figure 3b**), providing an additional role for cooperation within the crystal system.

3.2.Hirshfeld Surface Analysis

Using the Crystal Explorer software, we have identified the Hirshfeld surfaces [43] and their corresponding fingerprint plot [44], allowing us to analyze the intermolecular interactions between hydrogenfumarate and 4-phenylpiperazine-1-ium and calculate the percentage of each non-covalent interactions in 4PPHFUM through 2D fingerprint mapping. This software allows us to establish the d_{norm} mode, which is a 3D cartography of the various non-covalent interactions that can be observed in molecular crystals. These interactions can be spotted through the color combinations of blue, white and red, which respectively stand for: Interatomic interaction > van der Waals radius (refers to atomic repulsion), Interatomic interaction = vdW radius and Interatomic interaction < vdW radius (stands for hydrogen bonding).

As shown in **Figure 4**, O...H/H...O contacts (29 %) which refer to O-H…O, N-H...O and C-H...O hydrogen bonds and C…H/H…C contacts (18.3 %) that stand for C-H...π interactions account for 47.3 % of the non-covalent interactions in 4PPHFUM. This calculation result shows the strong interaction between these two organic molecules and therefore the high stability in the crystal system. H...H repulsive contacts account for a high percentage of 45 %,

this result is predicted, as organic molecules are rich in hydrogen atoms. The other remaining contacts H...N/N...H, C...O/O...C, C...C and O...O, represent a total of 7.4%.

3.3. HOMO-LUMO properties of 4PPHFUM

The HOMO and LUMO represent the Highest-Occupied and Lowest-Unoccupied Molecular Orbitals respectively. HOMO is associated to the ability of a molecule to donate an electron, in contrast to LUMO, which provides information on the electron acceptor character of the molecule [45]. The gap value ΔE($\Delta E = |E_{HOMO} - E_{LUMO}|$) is the absolute difference in energy between the frontier molecular orbitals, which expresses the reactivity of the compounds and is also a key factor in electrical conductivity [46,47]. In **Table 4**, we have listed the various reactivity parameters such as E_{HOMO}, E_{LUMO}, E_{Gap}, electronic affinity, electrophilicity, ionization potential, electronegativity, chemical potential, Hardness and Softness.

Figure 5 illustrates both the HOMO and LUMO orbitals of 4PPHFUM, the red and green paint colors mark the positive and negative signs, in each case, of the molecular orbital wave function. HOMO orbitals are clustered on the 4-phenylpiperazine-1-ium cation, in contrast to the LUMO orbitals are concentrated on the hydrogenfumarate anion. We can therefore deduce that the hydrogenfumarate anion act as an electron acceptor, while 4-phenylpiperazine-1-ium acts as an electron donor.

The energy gap between the HOMO (-5.9250 eV) and LUMO (-2.5551 eV) orbitals provides the Gap energy, which stands at 3.37 eV, attesting that 4PPHFUM is a semiconductor.

3.4. Molecular Electrostatic Potential (MEP) Surface

The MEP surface is a 3D topographical map of a molecule's charge distribution.This map is composed of three colors: red, blue and green, which respectively indicate the negative, positive and neutral regions, thus indicating the charge distribution in the molecule studied [48,49]. **Figure 6** shows the MEP surface of 4PPHFUM charted using quantum chemical computations. The red area is clustered over the hydrogenfumarate anion, whilst the blue region is packed over the 4-phenylpiperazine-1-ium cation. This precise coloration profile is typical of the relative donor-acceptor characteristics of the hydrogenfumarate anion and the ethyl ketal of the 4-phenylpiperazine-1-ium cation.This theoretical result is a convincing indication of the interaction that takes place between these two organic entities, and of the super complexation between them through the creation of non-covalent interactions.

3.5. Quantum Theory of Atoms in Molecules (QTAIM)

Atoms in Molecules is a quantum theory based on the fundamental fact that electron density plays an essential role in explaining and making sense of experimental observations in chemistry, this theory has been a major success in parallel with progress in the precision of X-ray crystallography [50]. QTAIM properties were mapped according to electron density at the critical binding point (BCP), the potential energy density at the BCP is strongly related to the hydrogen bond energies, π···π stacking interactions in benzene dimers are also related to BCP [50]. The following is a classification of hydrogen-bond interactions based on energy and topological data [51]:

- $|E_{HB}| < 12$ kcal.mol$^{-1,}$ $\nabla^2\rho(r) > 0$ and $H(r) > 0$: Weak H-bonds.
- 12 kcal.mol^{-1}< $|E_{HB}| < 24$ kcal.mol$^{-1,}$ $\nabla^2\rho(r) > 0$ and $H(r) < 0$: Medium-strength H bonds.
- $|E_{HB}| > 24$ kcal.mol$^{-1,}$ $\nabla^2\rho(r) < 0$ and $H(r) < 0$: Strong H-bonds.

The QTAIM results presented in **Table 5** and illustrated in **Figure 7** show that the attachment between the hydrogenfumarate anion and the 4-phenylpiperazine-1-ium cation within the asymmetric unit of 4PPHFUM is mediated purely by the N-H...O hydrogen bond, which is compatible with the results obtained from single-crystal X-ray diffraction data and also confirms the good agreement between the two types of results.

3.6. Reduced Density Gradient (RDG)

To help us make all non-covalent interactions more apparent using a visual tool, we applied reduced density gradient (RDG) theory, as shown in **Figure 8**. RDG electron density as a function of (sign (λ2)*ρ)) and iso-surface density offers revealing information concerning the nature and the intensity of the interactions that exist in the materials. The function of (sign (λ2)*ρ)) is located in the range [−0.05 a.u. - 0.05 a.u] of RDG's dispersion spectra, which are classified as follows [52,53]:

- H-bonding (displayed in blue): (sign (λ_2)*ρ))< 0
- vdW interactions (displayed in green): (sign (λ_2)*ρ)) close to 0
- Steric effects (displayed in red): (sign (λ_2)*ρ))>0

As illustrated below in **Figure 8.b**, the blue marks between the oxygen atom of the hydrogenfumarate anion and the hydrogen atoms of the 4-phenylpiperazine-1-ium cation indicate a very close interaction corresponding to the N-H...O hydrogen bond. The red spots at the center of the cation rings are caused by steric effects due to the repulsion between the

hydrogen atoms, while the van der Waals interactions that have been established between the anion and cation atoms individually are shown in green.

3.7. Molecular docking study of4PPHFUM as a Tyrosinase Inhibitor

Supramolecular chemistry has attracteda great deal of interest in chemical biology, with the aim of combining simple molecules to synthesize new ones, linked together by non-covalent interactions. This combination gives the new product the properties of the original reagents, as well as more interesting properties than the old ones.The creation of biomedicines through supramolecular chemistry has led to high performance in terms of interaction with proteins, inhibiting their functionalities and immobilizing them [54,55].

Molecular docking is a powerful technique for studying binding orientations and clarifying the molecular mechanisms of ligands in the active regions of the proteins concerned [56]. The 3D crystal structure of tyrosinase (2y9w) was extracted from the RCSB protein database, while the structures of fumaric acid, 1-phenylpiperazine, thiamidol, hydroquinone, resorcinol, hexylresorcinol and kojic acid were obtained from the PubChem database. Single-crystal X-ray diffraction data for 4PPHFUM were used for this analysis. Through the use of the iGEMDOCK program, the best docked positions of all ligands with protein tyrosinase (2y9w) were spotted and illustrated in Table 7, then plotted in **Figures 9** and **10** using Discovery Studio to show the best docking positions and the 3D interactions between the ligands and the protein.

Thiamidol, hydroquinone, resorcinol, hexylresorcinol and kojic acid are the best tyrosinase inhibitors available [57-59]. In this study, we used their structures in conjunction with the new compound 4PPHFUM to compare their interaction energies with tyrosinase.

Obviously, the novel compound 4PPHFUM has the widest interaction energy (in absolute value) with tyrosinase (99.0615kcal.mol^{-1}) than both its initial reactive product and all the other tyrosinase inhibitors listed last as shown in **Table 6** and **Figure 9**. The 3-D presentation (**Figure 10**) showing the highly enriching interactions between our compounds and tyrosinase, which are a combination of H-bonds, electrostatic interactions and pi-alkyl interactions. 4PPHFUM interacts with tyrosinase via three H-bonding interactions as shown: 4PPHFUM with UNK89 amino acid at a distance of 2.18 Å, the second is with amino acid ALA79 (2.18 Å) and the third with the amino acid GLU19 at a 2.64 Å spacing. This interaction is also supported by electrostatic and pi-alkyl interactions with the amino acids ARG94 and VAL92 at distances of 4.07 Å and 4.28 Å respectively.

This analysis confirmed the inhibition of tyrosinase by this new supramolecule, whose interaction energy is superior to that of all other single molecule with which it was compared. The deduction that should be a key encouragement for researchers is the role of non-covalent interactions in the synthesis of supramolecules with interesting properties.

4. Conclusion

A successful soft-chemistry synthesis strategy has enabled us to produce the new compound (4-phenylpiperazine-1-ium) hydrogenfumarate. Its creation was validated by structural analysis using X-ray diffraction on a single crystal. Crystal stacking is afforded through O-H...O, N-H...O and C-H...O hydrogen bonds, also aided by C-H...π interactions between organic cations, which were also confirmed and computed using Hirshfeld surface analysis. To deepen our understanding of this compound's specific characteristics, several DFT calculations were carried out. The therapeutic effect of 4PPHFUM as a tyrosinase inhibitor was investigated via molecular docking technique. Our assumption was supported by the result of the analysis, which showed the high interaction energy of this new material with tyrosinase, outperforming the most potent tyrosinase inhibitors. These findings suggest that a great deal of study should be done on the synthesis of these kinds of supramolecules in order to create a material that is useful in the intended sector and combines the qualities of the beginning reagents with additional, intriguing capabilities.

Acknowledgments: This study was supported by the Researchers Supporting Project no. RSP2023R61 of King Saud University, Riyadh, Saudi Arabia. This study was partially carried out within the state assignment no. 0287-548 2021-0012 for the Institute of Chemistry and Chemical Technology, Siberian Branch of the Russian Academy of Sciences.

References

[1] G.R. Desiraju, Crystal engineering: A brief overview, J. Chem. Sci., 122 (2010) 667-675.

[2] C.B. Aakeröy, M.E. Fasulo, J.Desper, Cocrystal or Salt: Does It Really Matter?,Mol. Pharm., 4 (2007) 317–322.

[3] M. Arshad, K. Ahmed, M Bashir, N. Kosar, M. Kanwal, M. Ahmed, H.U. Khan, S. Khan, A. Rauf, A. Waseem, T. Mahmood, Synthesis, structural properties and potent bioactivities supported by molecular docking and DFT studies of new hydrazones derived from 5-chloroisatin and 2-thiophenecarboxaldehyde, J. Mol. Struct., 1246 (2021) 131204.

[4] M. Jemai, N. ISSAOUI, T. Roisnel, A.S. Kazachenko, O.M. Al-Dossary, H.Marouani, Solvent–solute and non-covalent interactions on bis(4-Piperidinonium ethyl ketal) oxalate compound: DFT calculations and in silico drug-target profiling, J. Mol. Liq., 391 (2023) 123261.

[5] F.A. Al-Zahrani, M.N. Arshad, A.M. Asiri, T. Mahmood, M. A. Gilani, R.M. El-shishtawy, Chem. Cent. J., Synthesis and structural properties of 2-((10-alkyl-10H-phenothiazin-3-yl)methylene)malononitrile derivatives; a combined experimental and theoretical insight, 10 (2016) 13.

[6] R.Zetterström, Nobel Prize 1937 to Albert von Szent-Gyorgyi: identification of vitamin C as the anti-scorbutic factor, ActaPaediatr., 98 (2009) 915-919.

[7] R. Shimizu, T. Sonoyama, T. Fukuhara, A. Kuwata, Y. Matsuo, R. Kubota, Safety, Tolerability, and Pharmacokinetics of the Novel AntiviralAgentEnsitrelvirFumaric Acid, a SARS-CoV-2 3CL ProteaseInhibitor, in Healthy Adults, Antimicrob. Agents Chemother., 66 (2022).

[8] H. Mukae, H. Yotsuyanagi, N. Ohmagari, Y. Doi, T. Imamura, T. Sonoyama, T. Fukuhara,G. Ichihashi, T.Sanaki, K. Baba,Y. Takeda,Y.Tsuge,T.Ueharaf, A Randomized Phase 2/3 Study of Ensitrelvir, a Novel Oral SARS-CoV-2 3C-Like Protease Inhibitor, in Japanese Patients withMild-to-Moderate COVID-19 or Asymptomatic SARS-CoV-2n Infection: Results of the Phase 2a Part, Antimicrob. Agents Chemother., 66 (2022) 1403-1411.

[9] L. Gou, J. Lee, J. Yang, Y. Park, H.Zhou Y. Zhan, Z. Lu, Inhibition of tyrosinase by fumaric acid: integration ofinhibition kinetics with computational docking simulations, Int. J. Biol. Macromol., 105 (2017) 1663-1669.

[10] S.Zolghadria, A.Bahramia, M.T.H.Khanb, J. Munoz-Munozc, F. Garcia-Molinad, F. Garcia-Canovasd, A.A. Saboury, A comprehensive review on tyrosinase inhibitors, J. Enzyme Inhib. Med. Chem., 34 (2019) 279–309.

[11] S. Halaouli, M. Asther, K. Kruus, L. Guo, M. Hamdi, J.-C. Sigoillot, M. Asther, A. Lomascolo, Characterization of a new tyrosinase from Pycnoporus species with high potential for food technological applications, J. Appl. Microbiol., 98 (2005) 332–343.

[12] M.R. Loizzo, R. Tundis, F. Menichini, Natural and Synthetic Tyrosinase Inhibitors as

Antibrowning Agents: An Update, Compr. Rev. Food Sci. Food Saf, 11 (2012) 378-398.

[13] T.S.Chang, An Updated Review of Tyrosinase Inhibitors, Int. J. Mol. Sci. 10 (2009) 2440-2475.

[14] A. Sharma, S. Wakode, F. Fayaz, S. Khasimbi, F.H. Pottoo, A. Kaur, An Overview of Piperazine Scaffold as Promising Nucleus for Different Therapeutic Targets, Curr. Pharm. Des., 26 (2020) 4373-4385.

[15] T.F. Gomes, T.E.T. Pompeu, D.A. Rodrigues, F. Noël, R. Menegatti, C.H. Andrade, J.R. Sabino, E.S. Gil, T.D Costa, A.H. Betti, C.B. Antonio, S.M.K. Rates, C.A.M. Fraga, E.J. Barreiro, V.D. Oliveira, Biotransformation of LASSBio-579 and pharmacological evaluation of p-hydroxylated metabolite a N-phenylpiperazine antipsychotic lead compound, Eur. J. Med. Chem., 62 (2013) 214-221.

[16] R. Villanueva, Neurobiology of Major Depressive Disorder, Neural Plast., 2013 (2013) 873278.

[17] A.K. Rathi, R. Syed, H.S. Shin, R.V. Patel, Piperazine derivatives for therapeutic use: a patent review (2010-present), Expert Opin. Ther. Pat., 26 (2016) 777-797.

[18] L. Akl, A.A Abd El-Hafeez , T.M. Ibrahim, R. Salem, H.M.M. Marzouk, R.A. El-Domany, P. Ghosh, W.M. Eldehna, S.M. Abou-Seri, Identification of novel piperazine-tethered phthalazines as selective CDK1 inhibitors endowed with in vitro anticancer activity toward the pancreatic cancer, Eur. J. Med. Chem., 243 (2022) 114704.

[19] N. Szkaradek, A. Rapacz, K. Pytka, B. Filipek, A. Siwek, M. Cegła, H. Marona, Synthesis and preliminary evaluation of pharmacological properties of some piperazine derivatives of xanthone, Bioorg. Med. Chem, 21 (2013) 514-522.

[20] M. Taha, M. Irshad, S. Imran, S. Chigurupati, M. Selvaraj, F. Rahim, N.H. Ismail, F. Nawaz, K.M. Khan, Synthesis of piperazine sulfonamide analogs as diabetic-II inhibitors and their molecular docking study, Eur. J. Med. Chem., 141 (2017) 530-537.

[21] Z. Zhang, N.A. Dales, M.D. Winther, Opportunities and Challenges in Developing Stearoyl-Coenzyme A Desaturase-1 Inhibitors as Novel Therapeutics for Human Disease, J. Med. Chem., 57 (2014) 5039-5056.

[22] S. Konduri, J. Prashanth, V.Siva Krishna, D. Sriram, J.N. Behera, D. Siegel, K. P. Rao, Design and synthesis of purine connected piperazine derivatives as novel inhibitors of Mycobacterium tuberculosis, 30 (2020) 127512.

[23] M. Bassetto, P. Leyssen, J. Neyts, M.M. Yerukhimovich, D.N. Frick, M. Courtney-Smith, A. Brancale, Insilico identification, design and synthesis of novel piperazine-based antiviral agents targeting the hepatitis C virus helicase, Eur. J. Med. Chem., 125 (2017) 1115-1131.

[24] C.Dokuzparmak, F.O.Tuncay, S.B. Ozdemir, B.Kurnaz, I.Demir, A.Colak, S.SErdem,N.Yildirim, Newly synthesized piperazine derivatives as tyrosinase inhibitors: in vitro and in silico studies, J. Iran. Chem. Soc., 19 (2022) 2739–2748.

[25] G.Z. Tuğçe, Ş.Fatma S, S. Suhaib, O. İlkayErdoğan; B. Erden, Ç. Burcu, Novel Piperazine Amides of Cinnamic Acid Derivatives as Tyrosinase Inhibitors, Lett. Drug Des. Discov., 16 (2019) 36-44.

[26] İ.Değirmencioğlu, F.O.Tuncay, U.Cakmak, Y.Kolcuoglu, The synthesis of novel piperazine-benzodioxole substituted phthalocyanines and investigation of their α-amylase and tyrosinase inhibition properties, J. Organomet. Chem., 951 (2021) 122012.

[27] L. J. Farrugia, WinGX and ORTEP for Windows: an update, J. Appl. Cryst., 45 (2012) 849-854.

[28] G.M. Sheldrick, Crystal structure refinement with SHELXL. ActaCrystallogr., 71 (2015) 3–8.

[29] M. Jmai,S. Gatfaoui,N. Issaoui,T.Roisnel,A.S. Kazachenko,O. Al-Dossary,H. Marouani, A.S. Kazachenko, Synthesis, Empirical and Theoretical Investigations on New Histaminium Bis(Trioxonitrate) Compound, molecules, 28 (2023) 1931.

[30] H. Israr, N. Rasool,K. Rizwan,M.A. Hashmi,T. Mahmood,U. Rashid,M. Z. Hussein, M. N. Akhtar, Synthesis and Reactivities of TriphenylAcetamide Analogs for Potential Nonlinear Optical Material Uses, symmetry, 11 (2019) 622.

[31]N. Kosar, S. Noreen, K. Ayub, M. Imran, T. Mahmood, Structural, Non-linear optical response and ultraviolet transparency of superalkalis (Li3O, Na3O, K3O)-doped bowel shape silicon carbide nanoclusters, Inorg. Chem. Commun., 157 (2023) 111328.

[32] G. Ahmad, N. Rasool, M. U. Qamar, M.M. Alam, N. Kosar, T. Mahmood, M. Imran, Facile synthesis of 4-aryl-N-(5-methyl-1H-pyrazol-3-yl)benzamides via Suzuki Miyaura reaction: Antibacterial activity against clinically isolated NDM-1-positive bacteria and their Docking Studies, Arab. J. Chem., 14 (2021) 103270.

[33] S. Muthu a, G. Ramachandran, spectroscopic studies (FTIR, FT-Raman and UV–Visible), normal coordinate analysis, NBO analysis, first order hyper polarizability, HOMO and LUMO analysis of (1R)-N-(Prop-2-yn-1-yl)-2,3-dihydro-1H-inden-1-amine molecule by ab initio HF and density functional methods, Spectrochim. Acta A Mol. Biomol., 121 (2014) 394-403.

[34] M.M. Julie, T. Prabhu, E. Elamuruguporchelvi, F.B. Asif, S. Muthu, A. Irfan, Structural (monomer and dimer), wavefunctional, NCI analysis in aqueous phase, electronic and excited state properties in different solvent atmosphere of 3-{(E)-[(3,4-dichlorophenyl)imino]methyl} benzene-1,2-diol, J. Mol. Liq., 336 (2021) 116335.

[35]B. Amul, S. Muthu, M. Raja, S. Sevvanthi, Spectral, DFT and molecular docking investigations on Etodolac, J. Mol. Struct., 1195 (2019) 747-761.

[36]M. Thirunavukkarasu, G. Balaji, S. Muthu, B.R. Raajaraman, P. Ramesh, Computational spectroscopic investigations on structural validation with IR and Raman experimental evidence, projection of ultraviolet-visible excitations, natural bond orbital interpretations, and molecular docking studies under the biological investigation on N-Benzyloxycarbonyl-L-Aspartic acid 1-Benzyl ester, Chem. Data Collect., 31 (2021) 100622.

[37]A. Thamara, R. Vadamalar, M. Raja, S. Muthu, B. Narayana, P. Ramesh, R.R. Muhamed, S. Sevvanthi, S. Aayisha, Molecular structure interpretation, spectroscopic (FT-IR, FT-

Raman), electronic solvation (UV–Vis, HOMO-LUMO and NLO) properties and biological evaluation of (2E)-3-(biphenyl-4-yl)-1-(4-bromophenyl)prop-2-en-1-one: Experimental and computational modeling approach, Spectrochim. Acta A Mol. Biomol., 226 (2020) 117609.

[38] R. Dennington, T. Keith, J. Millam, GaussView, Version 5, Semichem. Inc, Shawnee Mission, KS, USA, 2009.

[39] M.J. Frisch, G.W. Trucks, H.B. Schlegel, G.E Scuseria, M.A Robb, J.R Cheeseman, G. Scalmani, V. Barone, B. Mennucci, G.A. Petersson and al. Gaussian 09, Revision C.01, Gaussian, Inc.: Wallingford, UK, 2009.

[40]J. Tirado-Rives, W.L. Jorgensen, Performance of B3LYP Density Functional Methods for a Large Set of Organic Molecules, J. Chem. Theory Comput., 4 (2008) 297-306.

[41] J. Bernstein, Polymorphism of L-glutamic acid: decoding the [alpha]-[beta] phase relationship via graph-set analysis, ActaCryst., B74 (1991) 1004-1010.

[42] C. Zhao, R.M. Parrish, M.D. Smith, P.J. Pellechia, C.D. Sherrill, K.D. Shimizu, Do Deuteriums Form Stronger CH−π Interactions, J. Am. Chem. Soc., 134 (2012) 14306−14309.

[43] M. A. Spackman, D. Jayatilaka, Hirshfeld surface analysis, CrystEngComm. 11 (2009) 19-32.

[44] M. A. Spackman, J. J. Mckinnon, Fingerprinting intermolecular interactions in molecular crystals, CrystEngComm, 4 (2002) 378-392.

[45] A. Y. Musa, A. A. H. Kadhum, A. B. Mohamad, A. A. B. Rahoma, H. Mesmari, Electrochemical and quantum chemical calculations on 4,4-dimethyloxazolidine-2-thione as inhibitor for mild steel corrosion in hydrochloric acid, J. Mol. Struct., 969 (2010) 233-237.

[46] M. Jemai, M. Khalfi, N. Issaoui, T. Roisnel, A.S. Kazachenk, O. Al-Dossary, H. Marouani, A. S. Kazachenko, Y. N. Malyar, Role of Non-Covalent Interactions in Novel Supramolecular Compound, Bis(4-phenylpiperazin-1-ium) Oxalate Dihydrate: Synthesis, Molecular Structure, Thermal Characterization, Spectroscopic Properties and Quantum Chemical Study, Crystals, 13 (2023) 875.

[47] S. Gatfaoui, N. Issaoui, S.A. Brandán, M. Medimagh, O. Al-Dossary, T. Roisnel, H. Marouani, A. S. Kazachenko, Deciphering non-covalent interactions of 1,3-Benzenedimethanaminium bis(trioxonitrate): Synthesis, empirical and computational study, J. Mol. Struct., 1250 (2022) 131720.

[48] E. Scrocco, J. Tomasi, Reactivity and Intermolecular Forces: An EuristicInterpretationby Means of Electrostatic Molecular Potentials, Adv. Quant. Chem. 11(1978) 115-193

[49] P. Thul, V.P. Gupta, V.J. Ram, P. Tandon, Structural and spectroscopic studies on 2-pyranones,Spectrochim. Acta 75 (2010) 251-260.

[50] C.F. Matta, R. J. Boyd, The Quantum Theory of Atoms in Molecules: From Solid State to DNA and Drug Design, Wiley-VCH, John Wiley, 2007.

[51] I. Rozas, I. Alkorta, J. Elguero, Behavior of Ylides Containing N, O, and C Atoms as Hydrogen Bond Acceptors, J. Am. Chem. Soc., 122 (2000) 1154-11161.

[52] S. Gatfaoui, N. Issaoui, A. S. Kazachenk, O. Al-Dossary, T. Roisnel, H. Marouani, Synthesis, characterization and identification of inhibitory activity on the main protease of COVID-19 by molecular docking strategy of (4-oxo-piperidinium ethylene acetal) trioxonitrate, J. King Saud Univ. Sci., 35 (2023) 102758.

[53] S. Gatfaoui, N. Issaoui, T. Roisnel, H. Marouani, A proton transfer compound template phenylethylamine: Synthesis, a collective experimental and theoretical investigations, J. Mol. Struct., 1191 (2019) 183-196.

[54] D.A. Uhlenheuer, K. Petkaua, L. Brunsveld,Combining supramolecular chemistry with biology, Chem. Soc. Rev., 39 (2010) 2817-2826.

[55] S. Sakamoto, K. Kudo, Supramolecular Control of Split-GFP Reassembly by Conjugation of β-Cyclodextrin and Coumarin Units, J. Am. Chem. Soc., 130 (2008) 9574-9582.

[56] M. Medimagh, C. Ben Mleh, N. Issaoui, A.S.Kazachenko,T.Roisnel, O. M. Al Dossary,H. Marouani, L.G. Bousiakoug, DFT and molecular docking study of the effect of a green solvent (waterand DMSO) on the structure, MEP, and FMOs of the 1-ethylpiperazine-1,4-diium bis(hydrogenoxalate) compound, J. Mol. Liq., 369 (2023) 120851.

[57] T. Mann, W. Gerwat, J. Batzer, K. Eggers, C. Scherner, H. Wenck, F. Stäb, V. J. Hearing, K.H. Röhm, L. Kolbe, Inhibition of Human Tyrosinase Requires Molecular Motifs Distinctively Different from Mushroom Tyrosinase, J. Invest. Dermatol., 138 (2018) 1601-1608.

[58] S.Ullah,S.Son,H.Y.Yun,D.H. Kim,P. Chun, H.R. Moon,Tyrosinase inhibitors: a patent review (2011-2015), Expert Opin. Ther. Pat., 26 (2016) 347-362.

[59] L. Kolbe, T. Mann, W. Gerwat, J. Batzer, S. Ahlheit, C. Scherner, H. Wenck, F. Stäb, 4-n-butylresorcinol, a highly effective tyrosinase inhibitor for the topical treatment of hyperpigmentation, 27 (2013) 19-23.